Quantum State Tomography of Nanostructures and the Non–Linear Heisenberg Nilpotent Lie Group Model of Quantum Information Processing

Walter Schempp
Lehrstuhl fuer Mathematik I
University of Siegen
57068 Siegen, Germany
schempp@mathematik.uni-siegen.de
http://www.walter-schempp.de

Successiuamente á tempi et tempi giongendo lume a lume.

- Giordano Bruno

Die Phoronomie ist die Logik der Physik.

- Gottfried Wilhelm Leibniz

La science cherche le mouvement perpétuel. Elle l'a trouvé; c'est elle–même.

- Victor Hugo

As a common and fundamental quantum–mechanical result, the interference fringe pattern can only be observed as long as one cannot distinguish in principle which path the quantum object took before entering the detector.

- Folklore

An Aussagefähigkeit und subtiler Wandlungsmöglichkeit ist die Lichtmetapher unvergleichlich.

- Hans Blumenberg

The best understanding of what one can see comes from theories of what one can't see.

- Steve Smale

The thought that the best understanding of what one can visualize comes from mathematical theories of what one can't see has been expressed in various different ways by different scientists, and is specifically supported by quantum physics and nanophotonics ([84], [85]).

The advent of quantum physics and nanophotonics requires to adopt an operational point of view in which quantum systems and their quantum informational contents are described in terms of measurable and controllable observables. The basic concept of quantum entanglement or non–local quantum cross–correlation is one of the global mirror peculiarities of quantum physics that contrast with classical physics and therefore has attracted great interest ([83]). Einstein himself used the word "telepathically" within the context of the non–local action of the metaplectic automorphisms of the non–local quantum cross–

International Journal of Computing Anticipatory Systems, Volume 19, 2006
Edited by D. M. Dubois, CHAOS, Liège, Belgium, ISSN 1373-5411 ISBN 2-930396-05-9

correlation function. While quantum entanglement can occur between separate degrees of freedom of a single particle, only interparticle quantum entanglement bears the properties of Einstein–Podolsky–Rosen–Bohm non–locality ([30], [47], [67], [73], [92]) that are essential for quantum information protocols ([25], [95]) controlling

- quantum computation
- quantum cryptography
- quantum teleportation

Quantum computation: If a computer is built which evolves according to the rules of quantum physics, it could be prepared in a superposition of the possible classical input states. In a sense it then processes the different inputs in a massively parallel manner, to produce a superposition of outputs. It is known already that this parallelism would enable a quantum computer to attack some problems which are intractable by principle on any classical computer.

Quantum cryptography: Here the exchange protocols of individual quantum systems between a pair of correspondents enables them to establish a shared random bit string, or key, which can then be used for the encryption of a secret message. The use of quantum states by the correspondents means that they can be sure as to whether or not an eavesdropper has been listening. No such guarantee exists if the correspondents exchange their key classically because classical information can be read without disturbing it in any way.

Quantum teleportation: Although photons are the fastest and most robust carriers of information, quantum states are fragile because interactions with other systems are able to disrupt and eventually destroy their subtle superposition properties. On the other hand, classical bits are more robust and easy to localize and store. The idea of quantum teleportation protocols is to effect the faithful transfer of an unknown quantum state through a potentially disturbing environment by using classical channel bits. The concept of quantum teleportation utilizes the non–local cross–correlation between an entangled pair of photons or massive particles to prepare a quantum system in a state, which forms the exact replica of an arbitrary unknown quantum state of a distant individual quantum system. If quantum computers become a reality, there could be a real demand for such a facility, as outputs from some machines might be needed as input for others.

The commonly accepted interpretive summary of the experiments for quantum teleportation with polarization entanglement measurements via non–linear interactions of optical sum frequency generation (SFG) for correlating the input quantum state and the cross–correlated twin photon pair is that the SFG process occurs only when the input laser pulse train and the single output photon wave packet overlap perfectly inside the non–linear SFG optical crystal. Then the desired cross–correlated photon pair can be produced by cutting the optical crystal at the SFG phase–matching angle. Although the perfect overlap happens to be true in various particular experimental arrangements, it seems that many fall victim to the logical fallacy of extending the results to *all* similar experiments of photonics. In fact, it is not an uncommon misconception to assume that in these types of twin photon interference experimental setups the photons must arrive at the beam splitter at the same time, which seems to imply that some type of classical local interaction was required

between two single photons meeting at the beam splitter and agreeing which path to go, or how to be polarized ([73]). Due to the indistinguishability of the various two–photon amplitudes describing the alternatives leading to a coincidence count by the detectors, the Hopf bundle model of quantum holography $\mathbf{S}_1 \hookrightarrow \mathbf{S}_3 \xrightarrow{\eta} \mathbf{S}_2$ with projective Hopf entangler η establishes that interference occurs in twin photon experiments even though the photons arrive at the beam splitter at much different times ([83]).

If a quantum computer is to work properly, it has to perform quantum error correction to protect quantum information against unavoidable noise. Quantum error correction protocols protect information stored in two–level quantum systems, called qubits, by rectifying errors with operations conditioned on the measurement outcomes. Owing to the fragility of quantum states, the presence of noise during both storage and entangling operations diminishes any gain achieved through the use of quantum information processing without error correction. For instance, the realization of long–distance quantum cryptography requires protection from the effects of noise in communication channels. Error correction protocols have been implemented in quantum holography utilizing quantum entanglement, in experiments of nuclear magnetic resonance phoronomy using the standard spin echo (SE) procedure, and recently in atomic–ion qubits confined to a linear multi–zone trap. An encoded one–qubit state is protected against spin–flip errors by means of a three-qubit quantum error–correcting code. The quantum error–correcting code is not a standard linear repetition error–correcting code of classical communication channels but a stabilizer code. It admits a stabilizer group with two generators which are threefold tensor products of Pauli spin operators acting on the compact unit sphere

$$\mathbf{S}_3 \cong \mathbf{SU}(2, \mathbf{C})$$

in the vector space $\mathbf{R}^4 \cong \mathbf{C}^2$ underlying the skew field $\mathbf{H}$ of quaternions ([97], [18], [65]). The primary qubit state is corrected on the basis of the ancillae measurement outcome. It is noteworthy that any of an infinite sequence of qubit errors can be corrected by means of a finite set of unitary linear operations conditioned on measurement and control.

Within the context of the symmetries underlying the polarization entanglement measurements of quantum informatics, the idea of holography continues to attract much interest, especially as demands for high–capacity, high–speed storage and processing continue to grow ([75], [76]). There are several reasons quantum holography still stands out as a viable alternative to conventional technology. First, holographic storage is using multiple dimensions and offers, therefore, a potentially very high capacity which conventional magnetic and semiconductor memories cannot achieve presently. Second, holographic information may be accessed and processed in parallel, which for conventional devices is another challenging task not realized today. Finally, quantum holography provides the conceptional background for quantum entanglement and quantum lithography ([11], [22]).

Entangled quantum states involving photons or massive particles have been generated by various experimental means. In addition, fundamental quantum gates and a number of algorithms have also been demonstrated using these quantum structures and devices of quantum informatics. It is an interesting feature that quantum holography allows the visibility of the interference fringe pattern to be larger for an entangled twin photon state than is allowed by classical electromagnetic theory. This fact underlines the significance of laser–

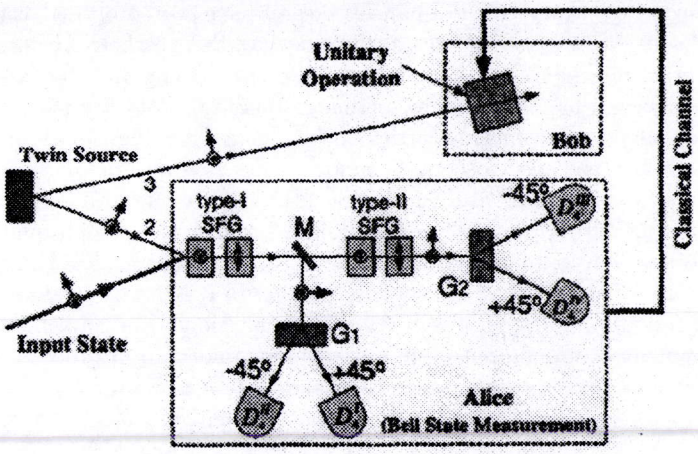

Figure 1: Schematic experimental setup for quantum teleportation with polarization entanglement measurements via non–linear interactions of optical sum frequency generation (SFG) for correlating the input quantum state and the entangled twin pair. The setup satisfies the conditions of an ideal quantum teleportation experiment: (i) the input quantum state is an arbitrary polarization state, (ii) the output quantum state forms an instantaneous copy of the input polarization state due to the symmetry of the configuration, (iii) the polarization entanglement measurement performed by Alice is able to distinguish the complete set of the four orthogonal Bell states by means of the oriented quadruplet of detectors $\{D^I, D^{II}, D^{III}, D^{IV}\}$ so that the input polarization state can be teleported with certainty, and (iv) for any input polarization state the teleportation procedure is a deterministic and not a probabilistic process, so that Bob can perform unitary linear operations on his twin particle after having learned from Alice through a classical communication channel which of her four detectors $\{D^I, D^{II}, D^{III}, D^{IV}\}$ has triggered. The polarization analyzer in front of Bob's detector demonstrates the spin echo (SE) half–cycle phase shifts of the oppositely oriented detector configurations $\{D^I, D^{II}\}$ and $\{D^{III}, D^{IV}\}$. The entangled twin pair shared by Alice and Bob is prepared by means of a spontaneous parametric down conversion non–linear optical crystal. The non–linear SFG optical crystals are pumped by femtosecond (fs) laser pulses. The first type–I SFG optical crystal converts two vertically polarized photons into a single horizontally polarized photon. Likewise, the second type–I SFG optical crystal converts two horizontally polarized photons into a single vertically polarized photon. Similarly, the other two Bell states are distinguished by the type–II SFG optical crystals. What is teleported inside the beam splitter experimental setup is the qubit associated with this single photon. The symbols $\odot$ and $\updownarrow$ indicate the respective horizontal and vertical orientations of the optical axes of the SFG optical crystals of type–I and type–II (M denotes a dichroic beam splitting mirror, $\{G_1, G_2\}$ act as holographic 45° polarization projectors).

driven high technologies and the mathematical models of rotational coherence spectroscopy experiments.

Recently, semiconductor quantum dot nanostructures have been proposed as the basic building blocks for solid–state based quantum logic devices due to their advantages, including the existence of an industrial base for semiconductor processing and the ease of integration with existing devices ([64], [98]). Semiconductor quantum dots are nanoscopic quantum structures that allow electronic properties to be tailored through quantum confinement. Advances in in coherence spectroscopy techniques have revealed the distinctive features of these nanostructures, including atomic like spectra with discrete and extraordinarily sharp spectral lines ([10], [40]). However, the similarities between atoms and quantum dots suggest the possibility of even greater opportunities ([108]). More specifically, one can consider the possibility of using coherent optical interactions to coherently engineer the quantum physical wave function. Such proposals have been envisioned for implementations of various schemes for quantum computation and coherent information processing and transfer protocols in which it is important to address and coherently control individual quantum units. In this way, it will be possible to extend earlier demonstrations of coherent control of semiconductor heterostructures such as photocurrent and THz radiations to a single quantum dot.

The molecular–beam epitaxy grown quantum dots come with size variation despite serious efforts on size, shape, and position control in the last decade or so. A most recently proposed nano–fabrication technique, which represents a radical departure from conventional approaches, is utilization of biological objects, such as viruses, as nano–templates for the fabrication ([2]).

Since Wilhelm Conrad Roentgen's epochal imaging achievement, scientists have dreamt of being able to instantantenously visualize molecular structure with a temporal resolution less than a femtosecond (1 fs = 10^{-15}s), which is the characteristic time scale of fundamental physical and chemical changes on an atomic length scale of 0.1 nanometer (1 nm = 10^{-9}m). Notice that in 1 fs light travels the remarkable short distance of about 3 μm (1 μm = 10^{-6}m). The idea of ultrafast science to control optical, physical and chemical processes in matter using the coherence properties of light appeared in the sixties in the scientific community. After a latent period of about two decades, coherent control of quantum physical processes and wave function engineering in sophisticated atomic and molecular systems have reached an advanced level of understanding including control of molecular chemical reactions, selective photodissociation of molecules, generation of non–classical motional states in ions, and localization of electronic wavepackets in atoms, molecules and solids, principally due to the advent of stable, flexible ultrafast laser sources ([75], [78], [82]). The broad spectral width of these pulse trains offers a wide range of applications. More recent work on coherent control has resulted in the full characterization of the amplitude and phase of an electronic wave function. These concepts have been extended to control the state of excitation in semiconductors including control of photocurrent direction and charge oscillations leading to THz radiation as indicated supra, as well as electron–phonon scattering, cyclotron emission, and population and orientation of excitons. In contrast to the higher dimensional semiconductor systems, the zero–dimensional quantum dots offer the possibility of coherent manipulation of a single localized quantum system in a way similar to that achieved in atoms but with the technological advantages of a solid–state system. The well–defined localized states of this system make it possible to use the results

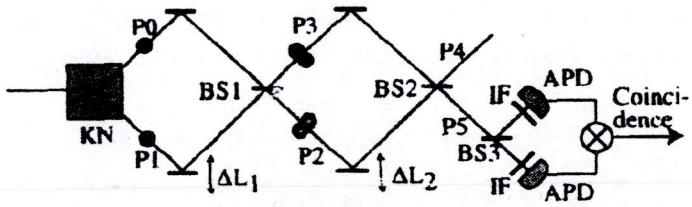

Figure 2: Schematic experimental setup for entangled photon pair or twin photon interference generated by parametric down–conversion and symmetrically positioned pinholes. The Heisenberg compact nilmanifold $N_{\mathbf{Z}}$ allows to model the optical crystal for entangled twin photon production. KN = $KNbO_3$ optical crystal, BS_j = 50:50 beam splitter, P_j = light path, ΔL_j = path length difference, IF = interference filter, APD = avalanche photodiode. The outcome of the laser–driven experiment indicates that the twin photon state exhibits the interference at a wavelength which is half of the wavelength of the one–photon state.

of coherent control in semiconductors to enable wave function engineering of specific target states, a result of both fundamental and practical significance.

While quantum optical investigations in the past have mostly performed with single atoms, more recently the combination between quantum holography and semiconductor nanostructures has emerged. Photons carry both spin and orbital angular momentum ([1]). The phenomenon of spin is associated with polarization and the orbital angular momentum with the azimuthal phase of the electric field ([51]). A photon can excite an electron in a semiconductor quantum dot nanostructure leaving behind a hole. The electron–hole pair, called the exciton, can also given an up or down spin orientation by the left–handed or right–handed circular polarization of laser light, repectively ([15], [64]). Apart of single quantum dots, semiconductor nanostructures can be incorporated into quantum well devices ([98]). Non–local cross–correlations between a photon and quantum states of the many–body carrier system of a semiconductor quantum well can be made visible by the interference fringe patterns arising from a single photon spontaneously emitted into different directions ([3]). These interference fringe patterns are realized by collecting light emitted from a quantum well into opposite directions and to combine those light beams on a common detector ([38]).

The system of electronic excitations in a semiconductor constitutes a complex many–body system with strong Coulomb interactions between the excited carriers. If one optically excites a planar semiconductor heterostructure by trains of fs laser pulses ([78]), the polarization and all the other quantum coherences dephase within tens of picoseconds (ps) due to scattering processes. Nevertheless, the system does not return to its ground state. The light emission from such an excited system is completely incoherent in the sense that the expectation value of the electric field vanishes. For normal mode emissions in the direction

of the quantization axis C given by the normal subgroup

$$\begin{pmatrix} 1 & 0 & z \\ 0 & 1 & 0 \\ 0 & 0 & 1 \end{pmatrix} \qquad (z \in \mathbf{R})$$

of the three–dimensional real Heisenberg nilpotent Lie group N consisting of the unipotent matrices

$$\begin{pmatrix} 1 & x & z \\ 0 & 1 & y \\ 0 & 0 & 1 \end{pmatrix} \qquad ((x,y),z) \in ((\mathbf{R} \oplus \mathbf{R}) \oplus \mathbf{R}),$$

however, interference effects are observable due to the strong quantum holographic light–matter correlations. The non–commutative multiplication law

$$\begin{pmatrix} 1 & x_1 & z_1 \\ 0 & 1 & y_1 \\ 0 & 0 & 1 \end{pmatrix} \begin{pmatrix} 1 & x_2 & z_2 \\ 0 & 1 & y_2 \\ 0 & 0 & 1 \end{pmatrix} = \begin{pmatrix} 1 & x_1 + x_2 & z_1 + z_2 + x_1 y_2 \\ 0 & 1 & y_1 + y_2 \\ 0 & 0 & 1 \end{pmatrix}$$

of the subgroup N of $\mathbf{SL}(3,\mathbf{R})$ with commutator

$$\left[\begin{pmatrix} 1 & x_1 & z_1 \\ 0 & 1 & y_1 \\ 0 & 0 & 1 \end{pmatrix}, \begin{pmatrix} 1 & x_2 & z_2 \\ 0 & 1 & y_2 \\ 0 & 0 & 1 \end{pmatrix} \right] = \begin{pmatrix} 1 & 0 & \det \begin{pmatrix} x_1 & x_2 \\ y_1 & y_2 \end{pmatrix} \\ 0 & 1 & 0 \\ 0 & 0 & 1 \end{pmatrix}$$

identifies $C \cong \mathbf{R}$ with the one–dimensional center of N. In addition, it displays an obvious lack of translational invariance along the in–line momentum carrying quantization axis C of the central extension

$$\boxed{\mathbf{R} \lhd N \longrightarrow \mathbf{R} \oplus \mathbf{R}} \tag{1}$$

This group extension of the symplectic plane N/C ([74], [54]), equipped with the action of

$$\mathbf{SL}(2,\mathbf{R}) \cong \mathbf{PMp}(2,\mathbf{R})$$

via the wedge product form of the plane $\mathbf{R} \oplus \mathbf{R}$

$$\wedge : \big((x_1,y_1),(x_2,y_2)\big) \rightsquigarrow \det \begin{pmatrix} x_1 & x_2 \\ y_1 & y_2 \end{pmatrix},$$

and the twofold covering group $\mathbf{Mp}(2,\mathbf{R})$ of metaplectic automorphisms are of central importance in imaging and quantum holography, as well as in the Kepplerian holographic imagery and high–precision rotational coherence spectroscopy of planetary orbits ([80]). The central group extension of the symplectic plane N/C reflects the circularity as well as the shift linearity of the three–dimensional real Heisenberg nilpotent Lie group N. Both principles, circularity combined with linearity, can be traced back to the philosophical work of the Renaissance–Neoplatonist Giordano Bruno (1548 to 1600). The automorphism group $\mathbf{Mp}(2,\mathbf{R})$ implies a phoronomic indistinctiveness which is basic for the characteristically inherent alternatives of quantum physics.

At the Lie algebra level, the non–commutatitivity of N is characterized by the Jacobi bracket of the real Heisenberg Lie algebra

$$\left[\begin{pmatrix} 0 & 1 & 0 \\ 0 & 0 & 0 \\ 0 & 0 & 0 \end{pmatrix}, \begin{pmatrix} 0 & 0 & 0 \\ 0 & 0 & 1 \\ 0 & 0 & 0 \end{pmatrix}\right] = \begin{pmatrix} 0 & 0 & 1 \\ 0 & 0 & 0 \\ 0 & 0 & 0 \end{pmatrix}.$$

The exponential map projects the center of the real Heisenberg Lie algebra

$$\left\{\begin{pmatrix} 0 & 0 & r \\ 0 & 0 & 0 \\ 0 & 0 & 0 \end{pmatrix} \mid r \in \mathbf{R}\right\}$$

onto the quantization axis C. At the level of the real vector space dual of the Heisenberg Lie algebra, the orbits of N under the coadjoint action of matrix

$$\begin{pmatrix} 1 & 0 & y \\ 0 & 1 & -x \\ 0 & 0 & 1 \end{pmatrix} \qquad ((x,y) \in \mathbf{R} \oplus \mathbf{R})$$

with respect to the dual basis

$$\left\{\begin{pmatrix} 0 & 0 & 0 \\ 1 & 0 & 0 \\ 0 & 0 & 0 \end{pmatrix}, \begin{pmatrix} 0 & 0 & 0 \\ 0 & 0 & 0 \\ 0 & 1 & 0 \end{pmatrix}, \begin{pmatrix} 0 & 0 & 0 \\ 0 & 0 & 0 \\ 1 & 0 & 0 \end{pmatrix}\right\}$$

geometrically represent the unitary dual $\hat{N}$ of N formed by the equivalence classes of all the irreducible unitary linear representations of N operating in an appropriate complex Hilbert space ([79]). The coadjoint orbits form a stack of pairwise entangled, inhomogeneous symplectic planes of frequency labels $\{(\nu, -\nu) \mid \nu \neq 0\}$ within the real vector space dual of the Heisenberg Lie algebra and oriented transversally to the frequency axis

$$\left\{\begin{pmatrix} 0 & 0 & 0 \\ 0 & 0 & 0 \\ \nu & 0 & 0 \end{pmatrix} \mid \nu \in \mathbf{R}\right\}.$$

These pairwise entangled, inhomogeneous symplectic planes of $\hat{N}$ form the substrate of the metaplectic automorphisms of the non–local quantum cross–correlation function associated with the central group extension $C \lhd N \longrightarrow \mathbf{R} \oplus \mathbf{R}$. The change of orientation performed by the central half–cycle reflection

$$\boxed{\nu \rightsquigarrow -\nu \qquad (\nu \neq 0)} \tag{2}$$

transversally to the stack of inhomogeneous symplectic planes along a meridian of the Bloch sphere or heavenly sphere $\mathbf{S}_2 = \eta(\mathbf{S}_3)$ of the concept of Hopf fibration $\mathbf{S}_1 \hookrightarrow \mathbf{S}_3 \xrightarrow{\eta} \mathbf{S}_2$ of phase circle $\mathbf{S}_1$, reflects the transition from right–handed to left–handed artificially structured materials or metamaterials. It also reflects the surface plasmon resonance in photonic crystals of negative refraction ([91], [109], [31], [37]) in the superlens problem of overcoming the diffraction limit of optical imaging ([71], [69], [27], [46], [85]). Because,

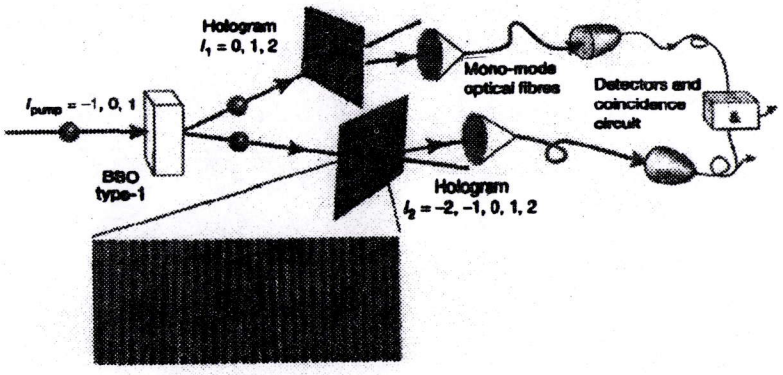

Figure 3: Schematic experimental setup for single photon mode detection. After parametric down–conversion, each of the photons enters a mode detector consisting of a computer generated hologram and a mono–mode optical fiber. The holograms are symmetrically positioned on the light paths. Two–photon quantum interference occurs for quantum correlated or entangled photon pairs even when two spatially separated interferometers are used.

loosely speaking, the concept of indistinguishability leads to interference, it is important to emphasize that the base manifold $\mathbf{S}_2$ of the Hopf bundle represents the indistinguishability of nanophotonics. Within this context, the Hopf projector η acts as a quantum entangler which maps the spinor rotation group $\mathbf{S}_3 \cong \mathbf{SU}(2, \mathbf{C})$ onto the compact sphere $\mathbf{S}_2$ in $\mathbf{R}^3$ ([90], [83]).

In addition, there is a homogeneous singular plane of frequency label $\nu = 0$ collecting pointwise in $\hat{N}$ the single characters of N. The characters of N are the one–dimensional unitary linear representations within the unitary dual $\hat{N}$ which play an important role in a laser–driven overtone procedure called high–order harmonic generation of instantaneous molecular structure imaging ([45]). In particular, according to Gerardus 't Hooft's reduction of dimensionality in quantum gravity, the combination of quantum physics and gravity requires the three–dimensional world to be an image of data that can be stored on a two–dimensional projection $\mathbf{R} \oplus \mathbf{R}$ along the dual quantization axis of $\mathbf{R} \lhd N \longrightarrow \mathbf{R} \oplus \mathbf{R}$ much like a hologram with no explicit mention of a longitudinal direction as in the super string realization of the holographic world ([101]).

In order to visualize the phenomenon of spin entanglement by the application of a half–cycle pulse in analogy to the refocusing pulse of the standard SE procedure of nuclear magnetic resonance imaging ([6], [81]), the inhomogeneous symplectic planes have to be organized in pairs of frequency labels $\nu \neq 0$ and $-\nu$.

The important point to make is that if the time scale is short compared with the time scale for loss of quantum coherence, the application of half–cycle pulses is suitable to generate quantum entanglement. In the other case, the atomic spin excitation by trains of half–cycle pulses ([72]) is able to produce by spectral resonances the rephasing effect of the standard

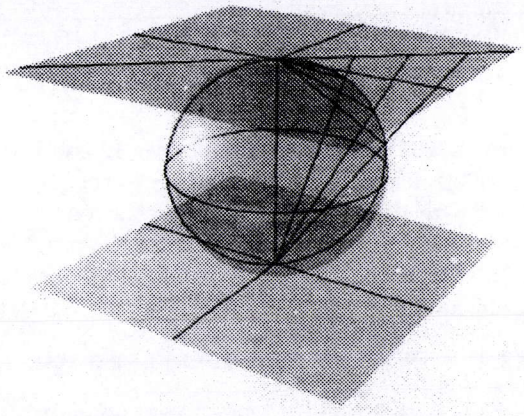

Figure 4: Visualization of spin entanglement by a half–cycle pulse which can be used as the operational pulse for the CROT gate. The CROT gate is equivalent to the standard CNOT gate of quantum information processing, but easier to realize as an all–optical quantum gate in a semiconductor quantum dot than the operations of the CNOT gate. Visualization of the magnetic field ramping in the unitary dual $\hat{N}$ and the two stereographic projections from the sphere of radius $\frac{1}{2}$ in $\mathbf{R}^3$ onto the Bloch sphere or heavenly sphere $\mathbf{S}_2 = \eta(\mathbf{S}_3)$ inside the central group extension $\mathbf{R} \lhd N \longrightarrow \mathbf{R} \oplus \mathbf{R}$, and the Hopf fibration $\mathbf{S}_1 \hookrightarrow \mathbf{S}_3 \xrightarrow{\eta} \mathbf{S}_2$ with projective Hopf entangler η. Its equatorial circle $\mathbf{S}_1$ of coherent phase control forms the intersection with the homogeneous singular plane $\nu = 0$ of the unitary dual $\hat{N}$ within the Heisenberg nilpotent Lie group model of laser–driven high–order harmonic generation from linear molecules, and can be identified with a maximal compact subgroup of $\mathbf{PMp}(2,\mathbf{R})$. The half–cycle reflections are performed transversally to the stack of inhomogeneous symplectic planes along the meridians of the Bloch sphere $\mathbf{S}_2 \hookrightarrow \mathbf{R}^3$. As in the case of the hologram the flat two–dimensional image is rich enough to code the full rotationally invariant description of three–dimensional objects. In the phoronomy of clinical magnetic resonance imaging, the basic tomographic configuration suggests the design of a vertical magnetic field generated by a twin pair of magnets in order to realize that the world is two–dimensional and not three–dimensional as previously supposed. In brane cosmology, a similar reflection construction provides the transition from the big crunch to the big bang metric singularity. It emphasizes the analogy between orbits and cosmologies.

SE procedure.

To observe and understand photon optical effects due to the quantized nature of light in a spin system, an ultracold cluster system, or a semiconductor system via the Heisenberg nilpotent Lie group model of quantum holography is a challenging goal of investigating quantum coherence by means of the unitary dual $\hat{N}$.

The transverse symplectic plane of projection along the quantization axis C of the Heisenberg nilpotent Lie group model is given by the coset

$$N/C \cong \mathbf{R} \oplus \mathbf{R}$$

and endowed with the symplectic structure

$$J_0 = \begin{pmatrix} 0 & -1 \\ 1 & 0 \end{pmatrix} \in \mathbf{SL}(2,\mathbf{R}) = \mathbf{Sp}(1,\mathbf{R}) \cong \mathbf{SU}(1,1,\mathbf{C}) .$$

The symplectic structure J_0 which is at the origin of the Einstein–Podolsky–Rosen–Bohm concept of non–locality ([92]) defines local coordinate systems on the plane $\mathbf{R} \oplus \mathbf{R}$ which are compatible with special relativity ([35]). Within this context, notice that the group $\mathbf{SL}(2,\mathbf{R})$ of automorphisms of N forms a double cover of the positive light cone preserving Lorentz subgroup $\mathbf{SO}_0(2,1)$, which is the identity component of the group $\mathbf{O}(2,1)$ of linear transformations preserving the Minkowski metric. Hence the isomorphisms

$$\mathbf{SO}_0(2,1) \cong \mathbf{PSL}(2,\mathbf{R}) , \qquad \mathbf{SO}_0(3,1) \cong \mathbf{PSL}(2,\mathbf{C}).$$

Combined with the covariance identity of the linear Schrödinger representation of N, they establish that the graphs of the non–local quantum cross–correlation functions are Lorentz–invariant.

Due to the circularity of N implemented by the one–parameter compact Cartan subgroup of $\mathbf{SL}(2,\mathbf{R})$,

$$\boxed{\{\exp 2\pi\nu J_0 t \mid t \in \mathbf{R}\} \cong \mathbf{T} \cong \mathbf{SO}(2,\mathbf{R})} \tag{3}$$

which acts in the natural way on the coset N/C, the symplectic structure J_0 of the plane $\mathbf{R}\oplus\mathbf{R}$ forms the basis of the rotational coherence spectroscopy of non–perturbative interactions. The tensor product of the neutral element of $\mathbf{SL}(2,\mathbf{R})$ with J_0 gives rise to the unitary linear transformation of matrix

$$\begin{pmatrix} 1 & 0 & 0 & 0 \\ 0 & 1 & 0 & 0 \\ 0 & 0 & 0 & -1 \\ 0 & 0 & 1 & 0 \end{pmatrix}$$

of the controlled rotation (CROT) gate of quantum information processing in the vector space $\mathbf{R}^4 \cong \mathbf{C}^2$ defined by the Hopf fibration $\mathbf{S}_1 \hookrightarrow \mathbf{S}_3 \xrightarrow{\eta} \mathbf{S}_2$ of a GaAs semiconductor quantum dot ([14], [55]). In a single dot, ultrafast control of spin excitions can be performed: The target bit is rotated through the half–cycle angle if and only if the control bit is 1. The transformation operates on the input wave function defined in the quantum computational basis and yields the output wave function.

Realized by a planar quantum well, the coset N/C generates equal probability for spontaneous emission of light along opposite path directions. Combining one light emission path from the left and one from the right corresponding to the associated circular and cocircular polarizations into a common detector leads to interference fringe patterns for fundamentally indistinguishable Clifford parallel paths. In the principal circle bundle model $N_{\mathbf{Z}}$ over the two–dimensional compact torus $\mathbf{T}^2$ they are implemented by paratactic Villarceau circle geometries ([9]) where the same in–plane momentum is transferred to the quantum well. The Villarceau circles of the bundle $N_{\mathbf{Z}}$, which acts in quantum optics as a non–linear photonic crystal or a two–dimensional lattice of spins ([92], [95], [101]), are helices of the torus ([57], [63]), that is, they intersect each meridian of $\mathbf{T}^2$ at a constant angle.

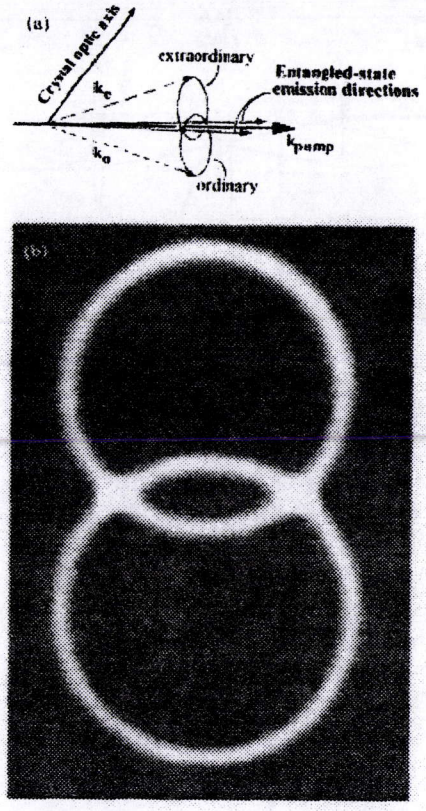

Figure 5: Clifford parallelism of paratactic Villarceau circle geometry and entangled quantum state generation by a photonic crystal without using an imaging lens. Measurement of the polarization state of one photon in the entangled twin pair of photon states defines the polarization state of the second photon instantaneously, whereas neither photon possesses its own well–defined polarization state before the measurement.

The three–dimensional Heisenberg compact nilmanifold $N_{\mathbf{Z}}$ represents a compactification of N which is constructed by means of three coordinate periodizations. The principal circle bundle $N_{\mathbf{Z}}$ carries the symmetric Poisson formula

$$\boxed{e^{\frac{1}{2}ixy}\sum_{n\in\mathbf{Z}} e^{iny}\bar{\mathcal{F}}f(n+x) = e^{-\frac{1}{2}ixy}\sum_{n\in\mathbf{Z}} e^{inx}f(n-y) \quad ((x,y)\in\mathbf{R}\oplus\mathbf{R})} \tag{4}$$

which reflects the circularity as well as the shift linearity of N. It allows to iteratively implement the quantum search algorithm on a database by means of quantum holographic spatial filtering ([7]). In the Poisson identity, as realized by linear shift registering Fourier optics, the signal f represents an element of the Schwartz space $\mathcal{S}(\mathbf{R})$ of rapidly decreasing

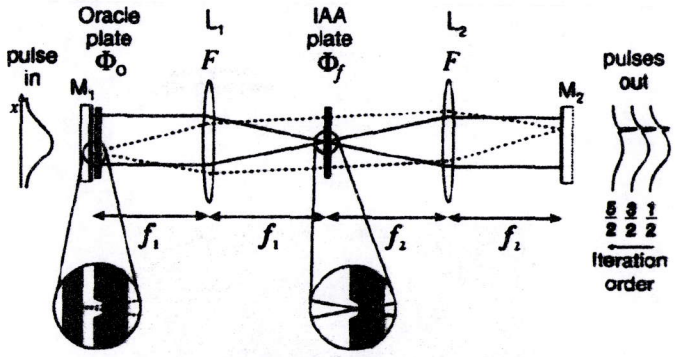

Figure 6: Quantum holographic implementation of the quantum search algorithm. A short laser pulse with a Gaussian transverse beam profile is launched into a cavity formed by two mirrors M_1, M_2. A line shaped depression in the oracle plate labels the item by imprinting a phase profile Φ_0. The inverted about the average amplitude operation performed by the IAA plate imprints a phase profile Φ_f in the Fourier plane of the oracle which is the homogeneous singular plane $\nu = 0$ of the unitary dual $\hat{N}$ within the Heisenberg nilpotent Lie group model of quantum holography. The fact that the focal lengths $f_1 \neq f_2$ of the spherical, achromatic doublet lenses can be chosen differently is sufficient to indicate that only interference, not entanglement, is used within the Heisenberg nilpotent Lie group model of quantum holography. The enlargements display planar cross–sections of the phase plates transverse to the laser beams. A high intensity peak, growing on the beam profile in the transverse output plane, indicates the sought item.

functions on the real time axis $\mathbf{R}$, or a tempered distribution $f \in \mathcal{S}'(\mathbf{R})$, and $\bar{\mathcal{F}} = \mathcal{F}^{-1}$ acts on the dual vector space $\mathcal{S}'(\mathbf{R})$ as the Fourier cotransform.

The periodic coordinates $(x, y) \in \mathbf{R} \oplus \mathbf{R}$ of the Poisson identity have been introduced into mathematical astronomy by Johannes Keppler through insistence on a literal interpretation of the Copernican hypothesis that the sun really was the immobile center of the planetary system, and by using collections of observations separated by 687 days, the period of the planet's revolution ([99], [80], [86]). Whenever it was, it was at the same place each time. This periodization procedure allowed Keppler, in effect, to observe the earth from a stationary Mars, by reversing the directions along which Tycho Brahe had observed the celestial positions of Mars from the earth. Based on such an ingenious protocol, the Imperial Mathematician succeeded in extending the phoronomy of planetary motions to a holographic imaging procedure of planetary orbits and to disprove the circular hypothesis of the physical Platonism inherent to Galileo Galilei's traditional reasoning of astronomical observations. It needed the ideas of another genius of first order, the mathematician and philosopher of rationalism in the age of enlightenment Gottfried Wilhelm Leibniz (1646 to 1716), to acknowledge the phoronomy as the logic of physics.

In the quantum search algorithm, each database item is associated with a quantum state. Initially the Fourier optical system is prepared in a linear superposition of all quantum

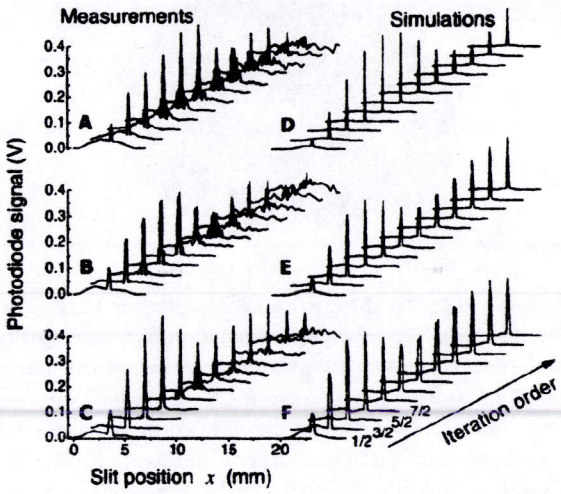

Figure 7: Iterative progress of the quantum search algorithm as shown by measured and simulated beam profiles. Oracle lines of widths (A) 42 μm, (B) 84 μm, and (C) 126 μm were used, corresponding to dadabases of 31.7, 15.8 and 10.6 items, respectively. Laser light coupled out of the cavity was recorded after each roundtrip through a scanning slit. The peak growing in the first iterations reveals the position of the sought item of the database. Computer simulations (D), (E), (F) have been performed using realistic experimental parameters, corresponding to the tempered distributions $f \in \mathcal{S}'(\mathbf{R})$ on the left hand side.

states of the database. A single laser pulse at the picosecond (1 ps = $10^{-12}s$) scale then enters a standing–wave cavity formed by two parallel mirrors. A so–called oracle labels the item by inverting the phase of the associated quantum state. As the pulse bounces back and forth between the two cavity mirrors, the transverse Gaussian beam profile being processed iteratively by the searching period of the marked items. A high intensity peak, growing on the beam profile in the transverse output plane, indicates the sought item. The protocol of efficiently finding "a needle in the haystack" by quantum holography does not require quantum entanglement ([62]). Indeed, quantum entanglement is neither necessary for the quantum search algorithm itself, nor for its efficiency. A quantum–over–classical reduction in the number of queries is achieved using only interference, not entanglement, within the Heisenberg nilpotent Lie group model of quantum holography.

Iteration by iteration, the light transmitted after each cavity roundtrip is imaged onto the movable slit of a linear shift register, coupled out and then collected on a photodiode in the output plane. The light pulses are short compared to the roundtrip period, so that a train of output pulses is obtained, one light pulse per iteration. The photodiode signal $f \in \mathcal{S}'(\mathbf{R})$ of the symmetric Poisson formula is amplified and recorded as a tempered distribution by a digitizing oscilloscope.

The concept of Clifford fiber parallelism of first and second kind has its origin in the Hopf

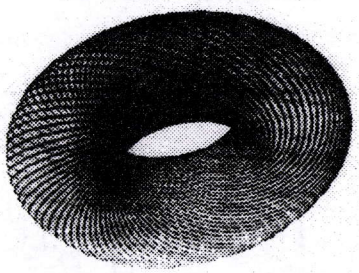

Figure 8: The exotic fibration of the three–dimensional Heisenberg compact nilmanifold $N_{\mathbf{Z}}$. The principal circle bundle $N_{\mathbf{Z}}$ over the two–dimensional compact torus $\mathbf{T}^2$ is obtained by circular, cocircular and transverse periodization along the quantization axis C of the three–dimensional real Heisenberg nilpotent Lie group N. The flat torus $\mathbf{T}^2$ carries paratactic Villarceau circles associated with the concept of Clifford fiber parallelism of first and second kind. They are helices of the torus, that is, the Villarceau circles intersect each meridian of $\mathbf{T}^2$ at a constant angle. The Bloch sphere or heavenly sphere $\mathbf{S}_2 = \eta(\mathbf{S}_3)$ arises from the space of fibers of the Hopf bundle which is topologically made up of two 2–discs glued together by a diffeomorphism of their boundaries. The metaplectic symmetry of the glueing process then leads to the geometric model of the cylindrical Dandelin–Quételet constellation of the Kepplerian planetary laws.

fibration

$$\begin{array}{ccc} \mathbf{S}_1 & \hookrightarrow & \mathbf{S}_3 \\ & & \downarrow \quad \eta \\ & & \mathbf{S}_2 \end{array}$$

where the projective Hopf entangler $\eta : \mathbf{S}_3 \longrightarrow \mathbf{S}_2$ denotes the canonical submersion with respect to the usual submanifold structures of the spheres, and $\mathbf{S}_1$ denotes the circle of phases. Then the magic map η is induced by the phase preserving stereographic projection $\mathbf{S}_3 \longrightarrow \mathbf{R}^3$ of the great circles of the compact sphere $\mathbf{S}_3 \cong \mathbf{SU}(2, \mathbf{C})$ in the vector space $\mathbf{R}^4 \cong \mathbf{C}^2$ which are the Clifford parallel orbits under the group action

$$\mathbf{R} \ni t \rightsquigarrow \left((w, w') \rightsquigarrow (e^{it}w, e^{it}w')\right)$$

on the vector space $\mathbf{R}^4 \cong \mathbf{C}^2$. For all other light paths no interference fringe pattern is observed because of the entanglement between the photon and quantum states of the many–body system.

In the experiment to establish quantum entanglement between a photon and a quantum well, a single quantum well consisting of a InGaAs layer embedded into a GaAs structure is mounted in a helium flow cryostat to maintain a temperature of 4 K and optically excited by means of a He–Ne laser so that photoluminescence could be collected from both sides of the quantum well. By moving the apertures vertically along a line perpendicular to the horizontal configuration plane of the interferometer, the experimental setup allows to combine photoluminescence emitted into two different forward and backward light paths. By adjusting the aperture such that only light emitted exactly perpendicular to the planar

quantum well structure is collected, a clear interference fringe pattern obtains on the screen ([101]).

The first important experimental result is that even a mesoscopic structure such as the quantum well device with its complex many–body dynamics does give rise to a clear interference fringe pattern for light spontaneously emitted in the mode direction normal to the quantum well plane. The interference fringe pattern rapidly vanishes by increasing the optical path difference. Interestingly and quite significantly, however, the interference fringe pattern disappears when the fundamental metaplectic symmetry of the three–dimensional real Heisenberg nilpotent Lie group N around the quantization axis C is broken by tilting the quantum well such that photoluminescence emission into opposite directions under a finite subtended angle is combined in the detector. As a consequence, the metaplectic group $\mathbf{Mp}(2,\mathbf{R})$ such that

$$\mathbf{PMp}(2,\mathbf{R}) \cong \mathbf{SL}(2,\mathbf{R})$$

governs quantum coherent two–body processes due to the non–local action of the metaplectic automorphisms of the non–local quantum cross–correlation function associated with the central group extension $C \lhd N \longrightarrow \mathbf{R} \oplus \mathbf{R}$. It follows that $\mathbf{Mp}(2,\mathbf{R})$ forms the symmetry group of the quantum entanglement experiment based on interfering photoluminescence emission ([106], [79], [66]).

A structural feature of harmonic analysis on the three–dimensional real Heisenberg nilpotent Lie group of utmost importance is the fact that $\mathbf{Sp}(1,\mathbf{R}) \cong \mathbf{SL}(2,\mathbf{R})$ acts as a group of automorphisms on the central group extension $C \lhd N \longrightarrow \mathbf{R} \oplus \mathbf{R}$. The covariant group system

$$(\mathbf{SL}(2,\mathbf{R}), N)$$

gives rise to the Galois correspondence of relativistic quantum field theory ([42], [43]). By lifting the covariance identity from the projective representations of $\mathbf{SL}(2,\mathbf{R})$ to the *bona fide* linear representations of the twofold cover $\mathbf{Mp}(2,\mathbf{R})$ of $\mathbf{SL}(2,\mathbf{R})$, the ensuing metaplectic symmetry of N around C suggests a coordinatization of the unitary dual $\hat{N}$ of N in terms of Plücker coordinates of the line geometry of the projective space $\mathbf{P}_3(\mathbf{R})$ because these are based on the in–line moments of coherent beams. Since the coherent emission process is included into the experimental setup, the relative phase between two light paths may not only be changed by varying the optical delay in one path but also by moving the spontaneously emitting quantum well. Therefore, in multiple quantum well structures the contrast of the interference fringe pattern can be controlled via the spacing d between the individual wells. If λ denotes the emission wavelength in the medium, the spacing $d = \frac{1}{2}\lambda$ provides the Bragg structure, and $d = \frac{1}{4}\lambda$ the anti–Bragg structure under mode emission in the normal direction of the planar quantum wells.

In conclusion, the quantum holographic model based on harmonic analysis on N establishes that the spontaneous emission of a complex many–body system such as a quantum well can give rise to a perfect interference fringe pattern if light emitted into appropriately chosen directions is combined in a detector. At the same time, light emitted into other directions does not lead to interference phenomena due to the entanglement between a photon and the quantum states of the carrier system. This quantum holographic experiment is in close analogy to the metaplectic "which–way" experiments of quantum optics. In

these experimental setups, the torque exerted by the phase dislocation onto the beam diffraction at the hologram provides polarization handedness of the single–photon modes ([57]). Whenever the carrier systems does not store information on the path of the light, full interference is observed. By simply tilting the sample, the carrier system can store information on the directionality of the light emission due to momentum conservation along the direction of the quantum well, and the interference fringe pattern vanishes. In contrast to metaplectic "which–way" experiments where a single light beam is split into two beams and by photonic tensor product interaction into four beams ([105]), the emitter is directly included into the experimental setup. The translational symmetry breaking automatically gives two indistinguishable paths for free, even under completely incoherent conditions, for spontaneously emitting stacks of quantum wells.

During the last two decades, atomic physics has undergone spectacular progress based on a new experimental method, called laser cooling and trapping. Laser cooling consists of using resonant exchanges of linear momentum between atoms and photons for reducing the momentum spread of a collection of molecules ([4]). Over the past few years many different approaches have been used to cool and trap molecules which are highly vibrationally excited ([110], [111], [34]). One major goal has been the creation of molecular Bose–Einstein condensates, which could lead to advances in molecular spectroscopy, studies of collisions, and precision tests of fundamental symmetries ([107]).

Recently, a new technique for creating ultracold molecule clusters led major advances towards molecular Bose–Einstein condensation. Ultracold atomic gases have become a medium to realize novel phenomena in condensed matter physics and test many–body theories in new regimes. The particle densities are 10^8 times lower than in solids, but at temperatures in the nanokelvin range, which are now routinely achieved, interactions and cross–corrrelations become important. Of particular interest are pairing phenomena in fermionic gases which have direct analogies to superconductivity. The fundamental metaplectic symmetry of N around the quantization axis C, expressed in terms of the twofold covering group $\mathbf{Mp}(2,\mathbf{R})$ of the group $\mathbf{SL}(2,\mathbf{R}) \cong \mathbf{Sp}(1,\mathbf{R})$ of automorphisms of N, brings in fascinating prospects for a controlled synthesis of ultracold tetramers in a single four–body quantum state in analogy to the foundation of ultracold dimers near atomic resonances ([19]). The ultracold dimers are created from an atomic Bose–Einstein condensate by ramping a magnetic field gradient and are levitated against gravity in a crosssed dipole trap formed by two CO_2 laser beams. The spherically symmetric CO_2 laser trap has a trapping frequency $\nu = 20$ Hz on the in–line momentum carrying quantization axis C, and a trapping depth of 7 μK. In this way, the tunability of the interactions in molecular quantum gases opens up the door to a new ultrafast laser–assisted cold and ultracold quantum chemistry which permits to determine the molecular structure in an instant by the laser–driven process of high–order harmonic generation in spatially aligned molecules ([77], [45], [53], [24]).

The technique of laser–driven high–order harmonic generation from a dense vapor of linear molecules requires only the measurement of the angular dependence of ion and harmonic signals, and opens the perspective to attosecond (1 as = 10^{-18}s) metrology in the regimes of extreme ultraviolet to soft X–ray coherent radiation ([3], [36], [68], [70], [88], [28]). In particular, molecular photonics does not require the sophisticated data processing protocols

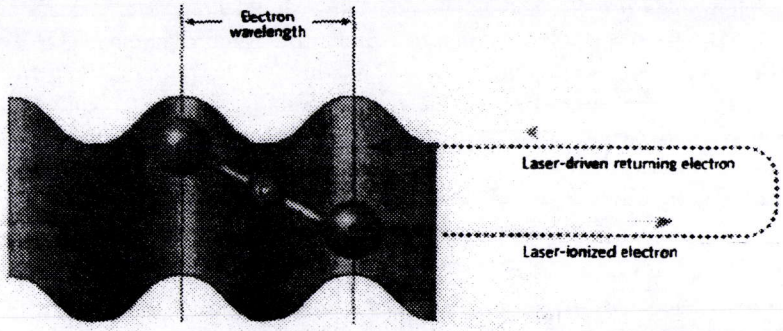

Figure 9: Laser–driven high–order harmonic generation of quantum holography and ultrafast science: The time–resolved measurement uses an intense near–infrared laser field to tear an electron from the orbitals of CO_2 molecules upon ionization. The laser field accelerates the electron and then drives it back towards the diatomic molecule a fraction of an optical cycle later. The recolliding electron recombines with the orbital of the molecule, giving up the energy it acquired as a single, soft X–ray photon within the same optical cycle. The laser–driven returning electron can be considered as a superposition of electron waves of different energy and momentum. An initial ultrafast laser pulse which excites a spinorial wavepacket in the molecules controls the spatial alignment of the molecule axes by a coherent superposition of quantum states. The spinorial wavepacket exhibits strong molecular–axis alignment along the quantization axis C, the center of the three–dimensional real Heisenberg nilpotent Lie group N, at regular periods of 5.4 ps in the case of a CO_2 molecule. A second, higher–intensity, ultrafast laser pulse generates coherent high–harmonic emission from molecules close to the maximum degree of spatial alignment. A strong interference modulation of the soft X–ray intensity is observed when the wavelength of the recolliding electron–wave resonantly matches the internuclear spacing between the two oxygen atoms within the linear CO_2 molecule. By precisely changing the time delay before the second laser pulse, the polarization projector onto the homogeneous singular plane $\nu = 0$ of the unitary dual $\hat{N}$ within the Heisenberg nilpotent Lie group model of laser–driven high–order harmonic generation from a dense vapor of linear molecules visualizes the coherent emission intensity for different magnitudes and angles of spatial alignment. The quantum holographic technique pinpoints the position of the atomic nuclei and complements tomographic reconstruction. By observing the emitted soft X–ray spectrum over a range of photon energies, it is possible to extract the position information from the laser–driven electron wave quantum holograms arising from different bond lengths on a time scale of a few fs.

of computerized tomography (CT) such as the Fourier slice theorem of the Radon transform $\mathcal{R}$ ([41]), or X–ray projection theorem:

$$\boxed{\mathcal{F}_{\mathbf{R}\oplus\mathbf{R}} f(\sigma\theta) = \mathcal{F}^1_{\mathbf{R}} \mathcal{R} f(\sigma, \theta) \qquad (\theta \in \mathbf{S}_1)} \tag{5}$$

The two–dimensional Fourier transform of the function f, evaluated on the homogeneous

line of inclination angle $\theta \in \mathbf{S}_1$, equals the one–dimensional Fourier transform of $\mathcal{R}f(\cdot, \theta)$ with respect to the first variable. Therefore, the Fourier slice theorem of CT technology lives on the the homogeneous singular plane $\nu = 0$ of high–order harmonic generation inside the unitary dual $\hat{N}$ of the three–dimensional real Heisenberg nilpotent Lie group N. In the helical version of modern multidetector row CT examinations at a preselected pitch, the patient transport is performed through the singular plane $\nu = 0$ of $\hat{N}$ within the equatorial circle $\mathbf{S}_1$ of the Bloch sphere $\mathbf{S}_2 \hookrightarrow \mathbf{R}^3$ which carries the multi–detector array.

The similarity of laser–driven high–order harmonic generation in atoms and small molecules extends to even larger organic molecules. Provided sufficiently short laser pulses of less than 100 fs duration are used, such molecules exhibit atomlike behaviour. However, unlike atoms, molecules are anisotropic systems. Consequently, processes such as multiphoton ionization can be strongly influenced by the angle subtended by the laser electric field vector and the molecular axis. In accordance to the Heisenberg nilpotent Lie group model of laser–driven high–order harmonic generation, experiments demonstrate that the single–molecule high–order harmonic generation response in a linear H_2^+ ion is enhanced if the laser field is linearly polarized perpendicular to the molecular axis ([102]).

A key parameter for a perfect levitation against gravity of the diatomic molecules is the precise value of their magnetic moment. The levitation field is crucial because the gravitational force is much stronger than the trapping force of the CO_2 lasers. Specifically it demonstrates that the Kepplerian holographic imagery and high–precision rotational coherence spectroscopy of planetary orbits is independent on the gravitational forces and only depends on the mechanism of spectral resonances ([80], [86]). To quote the cosmologist Bernard F. Schutz who emphasizes the methodological differences as follows:

Johannes Kepler (1571 to 1630) was the foremost mathematical astronomer of his time. Working in Prague, his detailed studies of the motions of the planets made it possible for him to show that the planets follow elliptical orbits with the sun always at one focus of the ellipse long before Newton explained this. The calculation was immense: more than a thousand sheets of arithmetic for his calculation of the orbit of Mars survive.

Unfortunately, Schutz does not recognize the symplectic aspects of Keppler's painstaking calculations ([87], [104]). Benoit Mandelbrot, the father of fractal geometry, describes the methodological differences in an even more concise style:

Newton konnte die Mechanik der Planetenbewegungen erklären, aber erst nachdem Keppler die Regeln für die Planetenbewegungen aufgeschrieben hat.

It is noteworthy that a familiar but incorrect version of the third Kepplerian planetary law asserts that the period is proportional to the $\frac{3}{2}$ power of the mean distance of the planet's position from the origin. In fact, the mean distance, that is the time average $\frac{\oint r(t)\,dt}{\oint dt}$, is *not* equal to the major semi–axis $a > 0$ of the elliptical orbit. However, it is interesting to note that the time average of the reciprocal distance $\frac{\oint \frac{1}{r(t)}\,dt}{\oint dt}$ is precisely $\frac{1}{a}$. Furthermore, it is noteworthy that the third Kepplerian planetary law has been discovered also by means of artificial intelligence ([50], [94]).

There exists a remarkable analogy between Einstein's misunderstanding of Schrödinger's concept of a "telepathic" non–local action underlying quantum entanglement, and the mis-

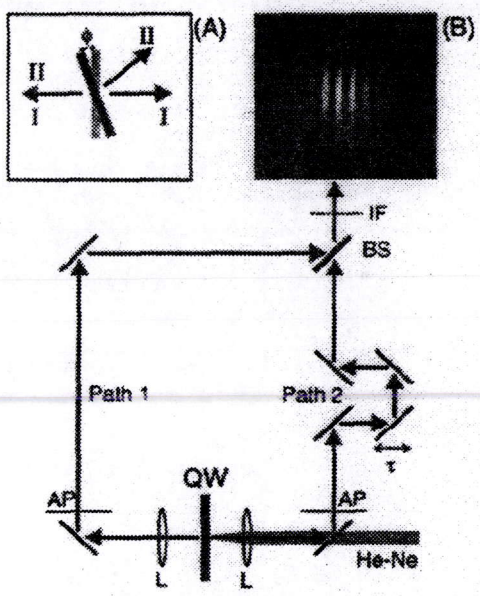

Figure 10: Schematic experimental setup suggested by the metaplectic "which–way" experiment for interfering photoluminescence emission from a single planar quantum well structure QW into different, metaplectically equivalent light paths inside the central group extension $\mathbf{R} \lhd N \longrightarrow \mathbf{R} \oplus \mathbf{R}$. The semiconductor QW is mounted in a helium flow cryostat to maintain a temperature of 4 K and optically excited by means of a He–Ne laser. Using two identical lenses L and apertures AP, the light paths are combined in a 50:50 beam splitter BS. The He–Ne laser pump beam was coupled through a dielectric mirror which reflects at the wavelength of the photoluminescence, yet transmits partially the wavelength of the He–Ne pump beam. An interference filter IF was placed in front of the charge coupled device (CCD) camera to cut off the reflected He–Ne pump beam. The optical path difference τ can be adjusted by an optical delay line. Inset B displays the spatial image of a typical interference fringe pattern measured with a cooled high sensitivity CCD camera. The fringes arising from a single photon spontaneously emitted into opposite path directions are obtained by introducing a small angle which is subtended by the two light paths. Inset A displays the measurement geometry for a tilted sample of tilt angle Φ. The interference fringe pattern for opposite emission under the subtended angle Φ is destroyed because then the different light paths have become fundamentally distinguishable by entanglement or non–local quantum correlation between the whole carrier system and the photon. In the actual experiment the tilt is achieved by moving the apertures AP on both sides perpendicular to the sample normal in accordance to the Heisenberg nilpotent Lie group model of quantum entanglement with the metaplectic symmetry of the three–dimensional real Heisenberg nilpotent Lie group N around the quantization axis C.

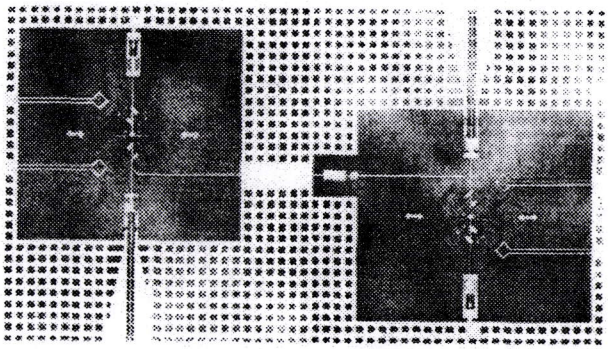

Figure 11: A condenser couples the two microchips of cogredient and contragredient orientations to form a quantum entanglement of its qubits by means of Josephson junctions.

understanding due to Galilei's physical Platonism of the scholastic "occult qualities" of the long distance action in space underlying the Kepplerian planetary laws. Because only coplanar orbit configurations are dynamically stable ([29], [100]), the tomographic approach to the Kepplerian planetary laws of extrasolar planetary systems evolving after an impulsive perturbation explains the apsidal resonances in which two elliptical orbits oscillate about a spatially aligned configuration with a small libration amplitude ([16], [17], [58]). In particular, extrasolar rotational coherence spectroscopy justifies the geometric model of the cylindrical Dandelin–Quételet configuration of the Kepplerian planetary laws under its metaplectic automorphisms ([13]). Extrasolar rotational coherence spectroscopy represents another step on the path directed to black hole quantum physics concerned with pair production in the presence of cosmological horizons ([12]). It confirms Murray Gell–Mann's statement:

Quantum mechanics is best and most fundamentally understood in the framework of quantum cosmology.

Selected parts of this article will be published in more detail as an invited paper in the forthcoming volume entitled *New Directions in Holography and Speckles*, H. John Caulfield and Chandra S. Vikram, Editors.

References

[1] L. Allen, M.J. Padgett, M. Babiker, The orbital angular momentum of light. In: Progress in Optics, Vol. 39, E. Wolf, Editor, pp. 291–372, Elsevier Science, Amsterdam 1999

[2] A.A. Balandin, V.A. Fonoberov, Vibrational modes of nano–template viruses. J. Biomed. Nanotech. 1, 90–95 (2005)

[3] A. Baltuška, Th. Udem, M. Uiberacker, M. Hentschel, E. Goulielmakis, Ch. Gohle, R. Holzwarth, V.S. Yakovlev, A. Scrinzi, T.W. Hänsch, F. Krausz, Attosecond control of electronic processes by intense light fields. Nature 421, 611–615 (2003)

[4] F. Bardou, J.–P. Bouchaud, A. Aspect, C. Cohen–Tannoudji, Lévy Statistics and Laser Cooling: How Rare Events Bring Atoms to Rest. Cambridge University Press, Cambridge, New York, Melbourne 2002

[5] S. Barreiro, J.W.R. Tabosa, Generation of light carrying orbital angular momentum via induced coherence gratings in cold atoms. Phys. Rev. Lett. 90, 133001–1 to 13301–4 (2003)

[6] M.A. Bernstein, K.F. King, X.J. Zhou, Handbook of MRI Pulse Sequences. Elsevier Academic Publishers, Amsterdam, Boston, Heidelberg 2004

[7] N. Bhattacharya, H.B. van Linden van den Heuvell, R.J.C. Spreeuw, Implementation of quantum search algorithm using classical Fourier optics. Phys. Rev. Lett. 88, 137901–1 to 137901–4 (2002)

[8] E. Binz, W. Schempp, Information technology: the Lie groups defining the filter banks of the compact disc. J. Comp. Appl. Math. 144, 85–103 (2002)

[9] A. Bloch, Sur les cercles paratactiques et la cyclide de Dupin. J. de Math. 3, 51–78 (1924)

[10] N.H. Bonadeo, J. Erland, D. Gammon, D. Park, D.S. Katzer, D.G. Steel, Coherent optical control of the quantum state of a single quantum dot. Science 282, 1473–1476 (1998)

[11] A.N. Boto, P. Kok, D.S. Abrams, S.L. Braunstein, C.P. Williams, J.P. Dowling, Quantum interferometric optical lithography: Exploiting entanglement to beat the diffraction limit. Phys. Rev. Lett. 85, 2733–2736 (2000)

[12] R. Brout, S. Massar, R. Parentani, Ph. Spindel, A primer for black hole quantum physics. Phys. Rep. 260, 329–446 (1995)

[13] J.E. Chambers, A hybrid symplectic integrator that permits close encounters between massive bodies. Mon. Not. R. Astron. Soc. 304, 793–799 (1999)

[14] G. Chen, N.H. Bonadeo, D.G. Steel, D. Gammon, D.S. Katzer, D. Park, C. Piermarocchi, L.J. Sham, Optically induced entanglement of excitons in a single quantum dot. Science 289, 1906–1909 (2000)

[15] P. Chen, C. Piermarocchi, L.J. Sham, Control of exciton dynamics in nanodots for quantum operations. Phys. Rev. Lett. 87, 067401–1 to 067401–4 (2001)

[16] E.I. Chiang, S. Tabachnik, S. Tremaine, Apsidal alignment in Upsilon Andromedae. Astron. J. 122, 1607–1615 (2001)

[17] E.I. Chiang, N. Murray, Eccentric excitation and apsidal resonance capture in the planetary system Upsilon Andromedae. Astrophys. J. 576, 473–477 (2002)

[18] J. Chiaverini, D. Leibfried, T. Schaetz, M.D. Barrett, R.B. Blakestad, J. Britton, W.M. Itano, J.D. Jost, E. Knill, C. Langer, R. Ozeri, D.J. Wineland, Realization of quantum error correction. Nature 432, 602–605 (2004)

[19] C. Chin, T. Kraemer, M. Mark, J. Herbig, P. Waldburger, H.–C. Nägerl, R. Grimm, Observation of Feshbach–like resonances in collisions between ultracold molecules. Phys. Rev. Lett. 94, 123201–1 to 123201–4 (2005)

[20] I. Chiorescu, Y. Nakamura, C.J.P.M. Harmans, J.E. Moij, Coherent quantum dynamics of a superconducting flux qubit. Science 299, 1869–1872 (2003)

[21] K.B. Cooper, M. Steffen, R. McDermott, R.W. Simmonds, S. Oh, D.A. Hite, D.P. Pappas, J.M. Martinis, Observation of quantum oscillations between a Josephson phase qubit and a microscopic resonator using fast readout. Phys. Rev. Lett. 93, 180401–1 to 180401–4 (2004)

[22] M. D'Angelo, M.V. Chekhova, Y.H. Shih, Two–photon diffraction and quantum lithography. Phys. Rev. Lett. 87, 013602–1 to 013602–4 (2001)

[23] W. Demtröder, Laser Spectroscopy: Basic Concepts and Instrumentation. Third Edition, Springer–Verlag, Berlin, Heidelberg, New York 2003

[24] M. Drescher, M. Hentschel, R. Kienberger, M. Uiberacker, V. Yakovlev, Th. Westerwalbesloh, U. Kleineberg, U. Heinzmann, F. Krausz, Time–resolved atomic inner–shell spectroscopy. Nature 419, 803–807 (2002)

[25] K. Edamatsu, R. Shimizu, T. Itoh, Measurement of the photonic de Broglie wavelength of entangled photon pairs generated by spontaneous parametric down–conversion. Phys. Rev. Lett. 89, 213601–1 to 213601–4 (2002)

[26] J. Eichler, G. Ackermann, Holographie. Springer–Verlag, Berlin, Heidelberg, New York 1993

[27] N. Fang, H. Lee, C. Sun, X. Zhang, Sub–diffraction–limited optical imaging with a silver superlens. Science 308, 534–537 (2005)

[28] A. Föhlisch, P. Feulner, F. Hennies, A. Fink, D. Menzel, D. Sanchez–Portal, P.M. Echenique, W. Wurth, Direct observation of electron dynamics in the attosecond domain. Nature 436, 373–376 (2005)

[29] E.B. Ford, V. Lystad, F.A. Rasio, Planet–planet scattering in the υ Andromedae system. Nature 434, 873–876 (2005)

[30] J.D. Franson, Bell inequality for positions and time. Phys. Rev. Lett. 62, 2205–2208 (1989)

[31] A. Grbic, G.V. Eleftheriades, Overcoming the diffraction limit with a planar left–handed transmission–line lens. Phys. Rev. Lett. 92, 117403–1 to 117403–4 (2004)

[32] H.S. Green, Information Theory and Quantum Physics: Physical Foundations for Understanding the Conscious Process. Springer–Verlag, Berlin, Heidelberg, New York 2000

[33] P. Griffiths, J. Harris, Principles of Algebraic Geometry. John Wiley & Sons, New York, Chichester, Brisbane 1978

[34] R. Grimm, A quantum revolution. Nature 435, 1035–1036 (2005)

[35] Ø. Grøn, Space geometry in rotating reference frames: A historical appraisal. In: Relativity in Rotating Frames, G. Rizzi, M.L. Ruggiero, Editors, pp. 285–333, Kluwer Academic Publishers, Dordrecht, Boston, London 2004

[36] M. Hentschel, R. Kienberger, Ch. Spielmann, G.A. Reider, N. Milosevic, T. Brabec, P. Corkum, U. Heinzmann, M. Drescher, F. Krausz, Attosecond metrology. Nature 414, 509–513 (2001)

[37] A.A. Houck, J.B. Brock, I.L. Chuang, Experimental observation of a left–handed material that obeys Snell's law. Phys. Rev. Lett. 90, 137401–1 to 137401–4 (2003)

[38] W. Hoyer, M. Kira, S.W. Koch, H. Stolz, S. Mosor, J. Sweet, C. Ell, G. Khitrova, H.M. Gibbs, Entanglement between a photon and a quantum well. Phys. Rev. Lett. 93, 067401–1 to 067401–4 (2004)

[39] M. Hübner, J. Kuhl, T. Stroucken, A. Knorr, S.W. Koch, R. Hey, K. Ploog, Collective effects of excitons in multiple–quantum–well Bragg and anti–Bragg structures. Phys. Rev. Lett. 76, 4199–4202 (1999)

[40] N.E. Hurt, Mathematical Physics of Quantum Wires and Devices. Kluwer Academic Publishers. Dordrecht, Boston, London 2000

[41] J. Itatani, J. Levesque, D. Zeidler, H. Niikura, H. Pépin, J.C. Kieffer, P.B. Corkum, D.M. Villeneuve, Tomographic imaging of molecular orbitals. Nature 432, 867–871 (2004)

[42] P.E.T. Jorgensen, Integral representations for locally defined positive definite functions on Lie groups. Int. J. Math. 2, 257–286 (1991)

[43] P.E.T. Jorgensen, X.–C. Quan, Covariance group C^*–algebras and Galois correspondence. Int. J. Math. 2, 673–699 (1991)

[44] B. Julsgaard, J. Sherson, J.I. Cirac, J. Flurášek, E.S. Polzik, Experimental demonstration of quantum memory for light. Nature 432, 482–486 (2004)

[45] T. Kanai, S. Minemoto, H. Sakai, Quantum interference during high–order harmonic generation from aligned molecules. Nature 435, 470–474 (2005)

[46] S. Kawata, Nano–optics beyond the diffraction limit. In: Fontiers of Nanoscience, 9th Japanese–German Symposium, pp. 49–69, JSPS Bonn Office 2005

[47] Y.–H. Kim, S.P. Kulik, Y.H. Shih, Quantum teleportation of a palarization state with a complete Bell measurement. Phys. Rev. Lett. 86, 1370–1373 (2001)

[48] W. Koechner, Solid–State Laser Engineering. 5th Edition, Springer–Verlag, Berlin, Heidelberg, New York 1999

[49] T. Kreis, Holographic Interferometry. John Wiley & Sons, New York, Chichester, Weinheim 2005

[50] P. Langley, Rediscovering physics with BACON.3. Proceedings of the Sixth International Conference on Artificial Intelligence, pp. 505–507 (1979)

[51] J. Leach, M.J. Padgett, S.M. Barnett, S. Franke–Arnold, J. Courtial, Measuring the orbital angular momentum of a single photon. Phys. Rev. Lett. 88, 257901–1 to 257901–4 (2002)

[52] Y.–S. Lee, T.B. Norris, M. Kira, F. Jahnke, S.W. Koch, G. Khitrova, H.M. Gibbs, Quantum correlation and intraband coherences in semiconductor Cavity QED. Phys. Rev. Lett. 83, 5338–5341 (1999)

[53] M. Lein, N. Hay, R. Velotta, J.P. Marangos, P.L. Knight, Role of the intramolecular phase in high–harmonic generation. Phys. Rev. Lett. 88, 183903–1 to 133903–4 (2002)

[54] J. Lepowsky, Perspectives on vertex operators and the monster. Proc. Symp. Pure Math. Vol. 48, 181–197 (1988)

[55] X. Li, Y. Wu, D. Steel, D. Gammon, T.H. Stievater, D.S. Katzer, D. Park, C. Piermarocchi, L.J. Sham, An all–optical quantum gate in a semiconductor quantum dot. Science 301, 809–811 (2003)

[56] H. Maeda, T.F. Gallagher, Nondispersing wave packets. Phys. Rev. Lett. 92, 133004–1 to 133004–4 (2004)

[57] A. Mair, A. Vaziri, G. Weihs, A. Zeilinger, Entanglement of the orbital angular momentum states of photons. Nature 412, 313–316 (2001)

[58] R. Malhotra, A dynamical mechanism for establishing apsidal resonance. Astrophys. J. Lett. 575, L33–L36 (2002)

[59] D. Marr, Vision: A Computational Investigation into the Human Representation and Processing of Visual Information. W.H. Freeman, New York 1982

[60] J.M. Martinis, S. Nam, J. Aumentado, Rabi oscillations in a large Josephson–junction qubit. Phys. Rev. Lett. 89, 117901–1 to 117901–4 (2002)

[61] R. McDermott, R.W. Simmonds, M. Steffen, K.B. Cooper, K. Cicak, K.D. Osborn, S. Oh, D.P. Pappas, J.M. Martinis, Simultaneous state measurement of coupled Josephson phase qubits. Science 307, 1299–1302 (2005)

[62] D.A. Meyer, Sophisticated quantum search without entanglement. Phys. Rev. Lett. 85, 2014–217 (2000)

[63] G. Molina–Terriza, J.P. Torres, L. Torner, Management of the angular momentum of light: Preparation of photons in multidimensional vector states of angular momentum. Phys. Rev. Lett. 88, 013601–1 to 013601–4 (2002)

[64] A. Moliton, Optoelectronics of Molecules and Polymers. Springer–Verlag, New York, Heidelberg, Berlin 2005

[65] M.A. Nielsen, I.L. Chuang, Quantum Computation and Quantum Information. Cambridge University Press, Cambridge, New York, Melbourne 2000

[66] H. Opolka, Theta Functions and Communication Theory. Lecture Notes, Institut für Algebra und Zahlentheorie der Technischen Universität Braunschweig, Braunschweig 1996

[67] Z.Y. Ou, X.Y. Zou, L.J. Wang, L. Mandel, Observation of nonlocal interference in separated photon channels. Phys. Rev. Lett. 65, 321–324 (1990)

[68] N.A. Papadogiannis, B. Witzel, C. Kalpouzos, D. Charalambidis, Observation of attosecond light localization in higher order harmonic generation. Phys. Rev. Lett. 83, 4289–4292 (1999)

[69] C.G. Parazzoli, R.B. Greegor, K. Li, B.E.C. Koltenbah, M. Tanielian, Experimental verification and simulation of negative index of refraction using Snell's law. Phys. Rev. Lett. 90, 107401–1 to 107401–4 (2003)

[70] P.M. Paul, E.S. Toma, P. Breger, G. Mullot, F. Augé, Ph. Balcou, H.G. Muller, P. Agostini, Observation of a train of attosecond pulses from high harmonic generation. Science 292, 1689–1692 (2001)

[71] J.B. Pendry, Negative refraction makes a perfect lens. Phys. Rev. Lett. 85, 3966–3969 (2000)

[72] D.F. Phillips, A. Fleischhauer, A. Mair, R.L. Walsworth, M.D. Lukin, Storage of light in atomic vapor. Phys. Rev. Lett. 86, 783–786 (2001)

[73] T.B. Pittman, D.V. Strekalov, A. Migdall, M.H. Rubin, A.V. Sergienko, Y.H. Shih, Can two–photon interference be considered the interference of two photons? Phys. Rev. Lett. 77, 1917–1920 (1996)

[74] A. Polishchuk, Abelian Varieties, Theta Functions and the Fourier Transform. Cambridge University Press, Cambridge, New York, Melbourne 2003

[75] A. Rebane, Femtosecond time–and–space–domain holography. In: Trends in Optics, Research, Development and Applications, A. Consortini, Editor, pp. 165–188, Academic Press, San Diego, CA 1996

[76] A. Renn, U.P. Wild, A. Rebane, Multidimensional holography by persistent spectral hole burning. J. Phys. Chem. A 106, 3045–3060 (2002)

[77] F. Rosca–Pruna, M.J.J. Vrakking, Experimental observation of revival structures in picosecond laser–induced alignment of I_2. Phys. Rev. Lett. 87, 153902–1 to 153902–4 (2001)

[78] C. Rullière, Editor, Femtosecond Laser Pulses: Principles and Experiments. Second Edition, Springer Science+Business Media, New York 2005

[79] W. Schempp, Harmonic Analysis on the Heisenberg Nilpotent Lie Group, with Applications to Signal Theory. Pitman Research Notes in Mathematics Series, Vol. 147, Longman Scientific and Technical, London 1986

[80] W.J. Schempp, Zu Kepplers Conchoid–Konstruktion. Result. Math. 32, 352–390 (1997)

[81] W.J. Schempp, Magnetic Resonance Imaging: Mathematical Foundations and Applications. Wiley–Liss, New York, Chichester, Weinheim 1998

[82] W. Schempp, The Fourier holographic encoding strategy of symplectic spinor visualization. In: New Directions in Holography and Speckles, H.J. Caulfield, C.S. Vikram, Editors, American Scientific Publishers, Stevenson Ranch, California, 2007

[83] W. Schempp, Indistinguishability and quantum entanglement. Far–East Journal of Mathematics (to appear)

[84] W. Schempp, Spinor–orbit interaction in nanostructures: The spin Hall effect of spintronics. Current Nanoscience (to appear)

[85] W. Schempp, Nanophotonics: Making tunnel barriers unitarily transparent. With applications of mode analysis to superlensing and celestial physics. Current Nanoscience (to appear)

[86] W. Schempp, Die Abtastmethode der quantenfeldtheoretischen Tomographie: Johannes Kepplers harmonische Analyse und Synthese. Manuscript (to appear)

[87] B.F. Schutz, Geometrical Methods of Mathematical Physics. Cambridge University Press, Cambridge, London, New York 1980

[88] T. Sekikawa, A. Kosuge, T. Kanai, S. Watanabe, Nonlinear optics in the extreme ultraviolet. Nature 432, 605–608 (2004)

[89] D. Shale, Linear symmetries of free boson fields. Trans. Amer. Math. Soc. 103, 149–167 (1962)

[90] R.W. Sharpe, Differential Geometry: Cartan's Generalization of Klein's Erlangen Program. Springer–Verlag, New York, Berlin, Heidelberg 1997

[91] R.A. Shelby, D.R. Smith, S. Schultz, Experimental verification of a negative index of refraction. Science 292, 77–79 (2001)

[92] Y.H. Shih, C.O. Alley, New type of Einstein–Podolsky–Rosen–Bohm experiment using pairs of light quants produced by optical parametric down conversion. Phys. Rev. Lett. 61, 2921–2924 (1988)
[93] A.E. Siegman, Lasers. University Science Books, Mill Valley, California 1986
[94] H.A. Simon, The Sciences of the Artificial. The MIT Press, Cambridge, London 1981
[95] T.P. Spiller, Quantum information processing: Cryptography, computation, and teleportation. Proc. IEEE 84, 1719–1746 (1996)
[96] C.E. Springer, Geometry and Analysis of Projective Spaces. W.H. Freeman and Company, San Francisco, London 1964
[97] A. Steane, Multiple particle interference and and quantum error correction. Proc. R. Soc. Lond. A 452, 2551–2577 (1996)
[98] T. Steiner, Editor, Semiconductor Nanostructures for Optoelectronic Applications. Artech House, London 2004
[99] B. Stephenson, Kepler's Physical Astronomy. Princeton University Press, Princeton, New Jersey 1994
[100] T.F. Stepinski, R. Malhotra, D.C. Black, The Upsilon Andomedae systm: Models and stability. Astrophys. J. 545, 1044–101057 (2000)
[101] L. Susskind, The world as a hologram. J. Math. Phys. 36, 6377–6396 (1995)
[102] R. Velotta, N. Hay, M.B. Mason, M. Castillejo, J.P. Marangos, High–order harmonic generation in aligned molecules. Phys. Rev. Lett. 87, 183901–1 to 183901–4 (2001)
[103] C.M. Vest, Holographic Interferometry. John Wiley & Sons, New York, Chichester, Brisbane 1979
[104] J.R. Voelkel, The Composition of Kepler's *Astronomia nova*. Princeton University Press, Princeton, Oxford 2001
[105] P. Walther, K.J. Resch, T. Rudolph, E. Schenck, H. Weinfurter, V. Vedral, M. Aspelmeyer, A. Zeilinger, Experimental one–way quantum computing. Nature 434, 169–176 (2005)
[106] A. Weil, Sur certains groupes d' opérateurs unitaires. Acta Math. 111, 143–211 (1964); Collected Papers, Vol. III, pp. 1–69, Springer–Verlag, New York, Heidelberg, Berlin 1979
[107] J. Weiner, Cold and Ultracold Collisions in Quantum Microscopic and Mesoscopic Systems. Cambridge University Press, Cambridge, New York, Melbourne 2003
[108] A. Yacoby, M. Heiblum, D. Mahalu, H. Shtrikman, Coherence and phase sensitive measurements in a quantum dot. Phys. Rev. Lett. 74, 4047–4050 (1995)
[109] T.J. Yen, W.J. Padilla, N. Fang, D.C. Vier, D.R. Smith, J.B. Pendry, D.N. Basov, X. Zhang, Terahertz magnetic response from artificial materials. Science 303, 1494–1496 (2003)
[110] M.W. Zwierlein, C.A. Stan, C.H. Schunck, S.M.F. Raupach, S. Gupta, Z. Hadzibabic, W. Ketterle, Observation of Bose–Einstein condensation of molecules. Phys. Rev. Lett. 91, 250401–1 to 250401–4 (2003)
[111] M.W. Zwierlein, C.A. Stan, C.H. Schunck, S.M.F. Raupach, A.J. Kerman, W. Ketterle, Condensation of pairs of fermionic atoms near a Feshbach resonance. Phys. Rev. Lett. 92, 120403–1 to 120403–4 (2004)